JOC The Journal of Organic Chemistry
ARTICLE
pubs.acs.org/joc

Z/E Isomerism in N^{α}-N^{α}-Disubstituted Hydrazides and the Amidoxy Bond: Application to the Conformational Analysis of Pseudopeptides Built of Hydrazinoacids and α-Aminoxyacids

Philippe Le Grel,[*,†] Arnaud Salaün,[‡] Clémence Mocquet,[†] Barbara Le Grel,[†] Thierry Roisnel,[§] and Michel Potel[§]

[†]ICMV and [§]CSM, UMR CNRS 6226, Universite de Rennes I, 263 avenue du General Leclerc 35042 Rennes Cedex
[‡]CBMN, UMR 5248, 2 rue Robert Escarpit, 33 607 Pessac

S Supporting Information

ABSTRACT: We have investigated the Z/E isomerism of the hydrazide link (CO-NH-N) and amidoxy link (CO-NH-O). The study was first focused on small molecular models using NMR and X-ray diffraction. It allowed determination of simple NMR criterions to differentiate easily the Z and E forms, which were then applied to investigate the behavior of these links inside the corresponding oligomers. Our results concerning the hydrazide link corroborate pioneering work that had been done in the 1970s except in the case were it is located inside aza-β^3-cyclopeptides, where the old empirical rules failed to predict the right geometry of the link. The geometrical preference of the amidoxy bond is also unambiguously established and differs clearly from recent theoretical calculations. Our findings help rationalize the close self-organization ability of aza-β^3-peptides and α-aminoxypeptides, two recently described foldamers.

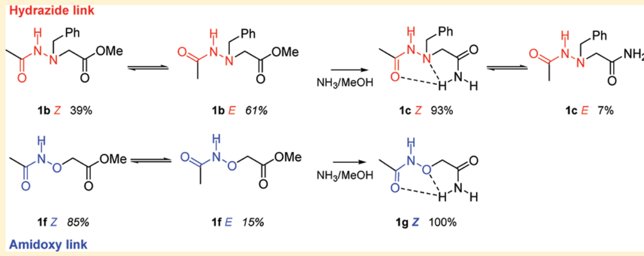

INTRODUCTION

Pseudopeptides are the subject of increasing attention as potential inducers of unnatural secondary structures, the so-called foldamers by S. H. Gellman.[1] The intramolecular H-bond networks that generally sustain the folded states in such biomimetic oligomers most often rely on amide to amide contacts, like in peptides themselves. To extend the foldamer concept, pseudopeptides with alternative polar groups have been synthesized, leading to the characterization of new folding patterns for ureapeptides[2] and α-amidoxypeptides.[3] α-Aminoxy-peptides (Figure 1, X = O) share a close structural relationship with aza-β^3-peptides (Figure 1, X = NR′),[4] an untypical kind of pseudopeptide in which side chains are attached on nitrogen atoms, as in peptoids[5] or azatides.[6] Yet, aza-β^3-peptides differ from the latter by the anchorage of side chains on pyramidal nitrogen atoms, acting as stereocenters. Despite the divergence in the location of chirality, the backbones of aza-β^3-peptides and α-aminoxypeptides show analogy in their folding propensity. Both sustain an intramolecular H-bond network that relies on recurrent C_8 pseudocycles.[7] The H-bond contact between hydrazide groups or amidoxy groups closes N−N and N−O turns, respectively. This backbone organization requires hydrazide and amidoxy groups to adopt a Z-conformation.

In peptides themselves, the extreme scarcity[8] of the E-conformation (*cis*-peptide bond) results from steric crowding. Even the simplest secondary amide, like N-methyl acetamide, will undergo a full shift of the Z/E isomerism associated with the double bond character of the amide bond toward the Z-form (Figure 2a). Interestingly, a recent theoretical approach calculated that a nonproline all-*cis* peptidic helix is not as energetically disfavored as one might expect provided that the *cis* amide groups slightly diverge from planarity.[9]

Z/E isomerism also occurs in hydrazide bonds, as established in the 1970s. However, the assignment of geometries and the identification of the governing parameters have been controversial. At the time, conclusions were drawn essentially by varying the polarity of solvents used for NMR analysis and reasoning on the respective steric crowding of the E and Z conformers by analogy with the amide bond.[10] Knapp was the first to perceive the drawbacks of this view and suggested that the Z/E equilibrium of hydrazide is not only governed by steric factors but also by the electronic repulsion that occurs between oxygen and nitrogen lone pairs occurring in the Z-form (Figure 2b).[11] Knapp's model was reinforced by the Z/E equilibrium observed in a new series of trisubstituted hydrazides synthesized by Perdicchia and Licandro.[12]

In contrast to the hydrazide linkage, to the best of our knowledge there is no experimental work concerning the conformational spectroscopic analysis of the amidoxy bond, except the theoretical approach recently performed by Wu on very simple molecular models to estimate the difference in energies

Received: July 13, 2011
Published: September 15, 2011

dx.doi.org/10.1021/jo201390b | J. Org. Chem. 2011, 76, 8756–8767

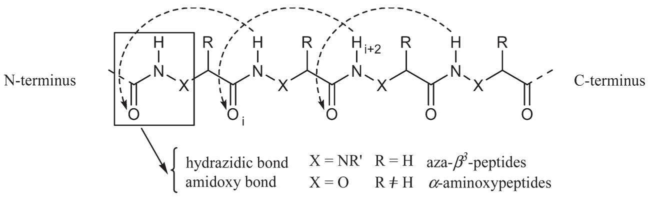

Figure 1. NH--OC H-bonding contacts in aza-β^3-peptides (X = NR′) and α-aminoxypeptides (X = O).

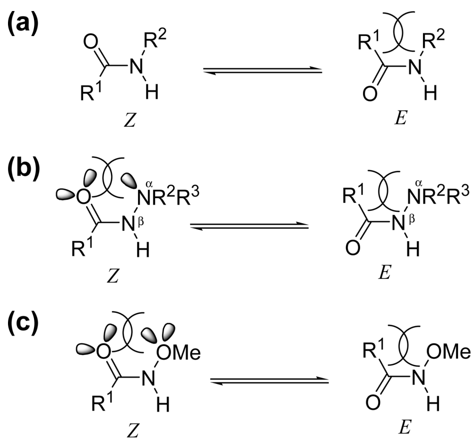

Figure 2. *Z*/*E* equilibrium of (a) primary amides, (b) the hydrazide bond, and (c) the amidoxy bond.

between the *E* and Z geometries.[13] The results of calculations predicted the *E*-form to be slightly favored in response to the electronic repulsion that occurs in the *Z*-form (Figure 2c), thereby supporting Knapp's hypothesis.

In this context, we decided to synthesize a series of model compounds to re-examine the geometrical preference of these amide surrogates. The work was specifically devoted to compounds in which the nitrogen atom linked to the carbonyl group is unsubstituted (NH, R^2 and $R^3 \neq$H), as these models reflect the nature of the hydrazide or amidoxy bonds in aza-β^3-peptides and α-aminoxypeptides. In this way, we planed to use the information gained from small molecular models to understand the behavior of hydrazide and amidoxy bonds in pseudopeptidic oligomers.

RESULTS AND DISCUSSION

Methods. Since the early studies of the hydrazide bond, NMR methods have gained considerable accuracy. At the time, NMR samples had to be quite concentrated with respect to the magnetic field. We could not find any information about the concentrations at which the ^{1}H NMR spectra were recorded or the chemical shift of the hydrazidic NHs in these pioneering studies. To reduce the influence of intermolecular H-bond contacts on chemical shift to negligible levels, ^{1}H NMR spectra were recorded at 10 mM (500 MHz, 298 K, $CDCl_3$ unless otherwise noted). The increased magnetic field, FT-NMR generalization, and the introduction of bidimensional experiments, for both the detection of scalar coupling or dipolar interactions, give direct insight into the conformation of molecules in solution. Special methods have also been developed to focus on the more versatile behavior of NH signals. For example, variation of chemical shift upon addition of increasing amounts of DMSO-d_6 were very informative in the study of H-bond contacts between polar groups.[14] These NMR tools have been combined for the present study, together with the $\Delta\delta$ analysis that we have developed a few years ago.[7c] Additionally, X-ray diffraction of crystallized samples was also performed for comparison with the analysis in solution.

***Z/E* Isomerism in N$^\alpha$,N$^\alpha$-Disubstituted Acetylhydrazides and Corresponding Oligomers.** Compound **1a** was first synthesized as a link to the pioneering works in that field as it was one of the first hydrazides to have been studied. At 298 K, the ^{1}H NMR spectrum of **1a** shows two sets of signals in a 3:1 ratio (Figure 3a, top). The methylene protons of the major isomer (74%) give an AB system with the hydrazidic NH as a sharp signal at 6.05 ppm. No diastereotopicity is observed for the minor conformer, for which the hydrazidic NH appears broad and flattened. A slight increase of the temperature to 318 K results in a better resolved NHz signal at 6.50 ppm while the AB system start to coalesce (Figure 3a, bottom).

It has been postulated that the diastereotopic signals should result from a hindered rotation around the N−N bond in the more crowded *E* isomer.[10b] Accordingly, using a more polar solvent to shift the equilibrium toward the more polar *Z* isomer leads to the lowering of the amount of the conformer associated with the diastereotopic signal. Evidence of this is shown in Figure 3b, recorded at 298 K in DMSO-d_6, where the percentage of the postulated *E* isomer is reduced to 57%. Both NH_Z and NH_E signals are strongly removed toward low field by DMSO, to which H-bonding occurs. This is in good agreement with the preclusion to establish intramolecular NH···OC bonds in all of the rotamers.

To probe these conclusions more definitively, we performed a NOESY experiment, which provides direct evidence of the *E* and *Z* geometries. This was made possible as both rotamers of hydrazide **1a** give sharp NHs singlets in DMSO-d_6. The NOESY pattern fully validates the postulated assignment, as only the minor isomer shows a strong NOE between the hydrazidic NH and the methyl group, which establishes its *Z* geometry (Figure 3b).

The recording of ^{1}H NMR spectrum of **1a** at 10 mM in $CDCl_3$ gives access to the chemical shift of nonhydrogen-bonded hydrazidic NHs in the *E* and *Z* geometries, which appear at 6.0 and 6.5 ppm, respectively. These reference values will be useful for the analysis to come.

Compound **1b** was then prepared to examine in which way the presence of a weak H-bond acceptor should affect the *Z*/*E* equilibrium relative to our reference compound. This compound also serves as a model for the C-terminus of aza-β^3-peptides ester (Figure 4, right) and will be useful for further discussion. Two sets of signals are still observable in the spectrum of **1b** (Figure 5). The *E* isomer (assigned using the above validated criteria of diastereotopicity) is still the major compound (61%), but its amount is lower when compared to **1a**. This agrees well with the presence of the more sterically demanding ester group. More notably, the chemical shifts of the hydrazidic NHs are shifted from around 1 ppm to lower fields (7.21 and 7.47 ppm for the *E* and *Z* rotamers, respectively). This can be reasonably interpreted as the result of a weak intramolecular H-bonding contact between the hydrazidic NH and the ester carbonyl group in each isomer, closing six-membered pseudorings (Figure 5).

Compound **1b** was then converted into **1c**. This chemical modification replaces the weak H-bond acceptor (the ester function) by the more polarized amide group but introduces concomitantly the amidic NH as a new H-bond donor. This

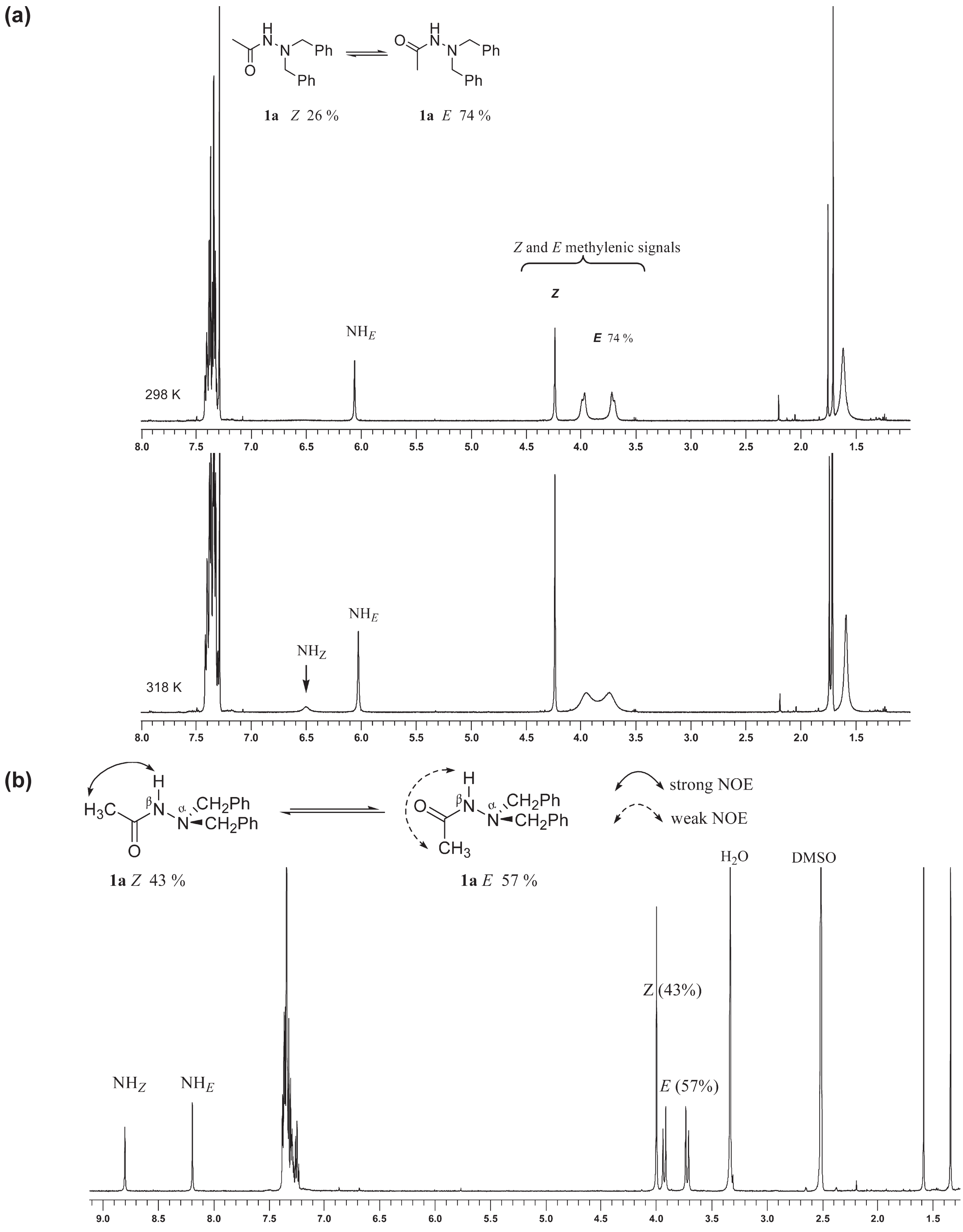

Figure 3. (a) (Top) ^{1}H NMR (500 MHz) spectrum of **1a** (T = 298 K/10 mM/$CDCl_3$). (Bottom) ^{1}H NMR (500 MHz) spectrum of **1a** (T = 318 K/10 mM/$CDCl_3$). (b) ^{1}H NMR (500 MHz; T = 298 K/10 mM) spectrum of **1a** in DMSO-d_6. The difference in NOEs allowing the Z and E conformation to be assigned to the rotamers of N,N-dibenzylacetydrazide **1a** are summarized on the equilibrium represented.

model compound reflects the internal hydrazidic linkage in aza-β^3-peptides (Figure 4, middle). The spectrum of compound **1c** shows two sets of signals in a 93:7 ratio (Figure 6). The major species shows no diastereotopic signals (associated with the E geometry) and a hydrazidic NH chemical shift of 6.52 ppm. This value, very close to those observed for **1a**, clearly signifies that the hydrazidic NH is not hydrogen bonded. In contrast, the amidic protons appear as two distinct signals with a chemical shift difference $\Delta\delta$ of 2.60 ppm.

In a previous article, we established that the discrimination of the NH resonance of a primary amide is observed in molecular models with internal H-bonding.[7c] Under these conditions, a composite averaged NMR signal results, with two equally resolved components of the same intensity. Briefly, the $\Delta\delta$ between the two components depends on the ratio between the folded state, where H-bonding discriminates the two amidic NHs ($\delta_{Hb} > \delta_{Hf}$) and the unfolded state, where they give a single signal (Figure 7).

We have already studied in detail the case of the closely related compound **1d** (Figure 4 left, and Figure 8 left), in which we concluded that the $\Delta\delta$ value of 2.60 ppm results from a bifurcated H-bond (N—N-turn), where the amide group interacts with both the lone pair of the N^{α} atom and the oxygen atom of the carbazidic carbonyl group. Given this information, it is asserted that the major conformer of **1c** corresponds to the *Z* isomer, where a similar arrangement can take place (Figure 8 right).

This interpretation is fully consistent with the NOESY data of **1c** where strong NOEs are observed between the hydrazidic NH and the methyl group as well as with both methylene groups. A medium NOE is also observed between the low field region of the composite amide signal, for which the major contribution corresponds to the NH_b proton and the methylene group of the acetamide moiety. These NOEs are summarized in Figure 9 (left). They parallel very well with interatomic distances measured on the X-ray structure of **1c** (Figure 9, right).

From the comparison between the data collected for **1a**, **1b**, and **1c**, it can be concluded that the formation of the H-bond in **1c** reverses the natural preference of the hydrazidic bond for the *E*-geometry, although the formation of the hydrazinoturn does not fully shift the equilibrium toward the Z-geometry. Actually, the signals of the minor conformer can reasonably be assigned to the *E* rotamer.

In the course of this comparative study, we have recorded the ^{13}C NMR and the 2D HMBC spectra for compounds **1a**, **1b**, and **1c**, from which we could determine the chemical shift of the carbonyl group for the *E* and *Z* rotamers (Table 1). The data shows that, despite the structural variations, like the presence or the absence of an H-bond, the chemical shifts remain homogeneous in each series, with the average values being significantly higher for the *E* rotamer (around 175 versus 169 ppm).

The HMBC experiment also shows that only the *E* isomer presents a $^{3}J_{CH}$ coupling between the hydrazidic NH and the carbon atom of the methyl group as illustrated in the case of **1b** in Figure 10. This is fully consistent with Karplus law, which validates undoubtebly the assignment of *E* and *Z* isomers. Similarly, it is well-known that $^{3}J_{HH}$ coupling constants are observable for the *E* isomer of the NHCHO fragment, the values for the *Z* isomer being very low and most often equal to zero.[15]

The above findings, obtained from small molecular models, were then expanded upon using the NMR data collected from our studies of aza-β^3-peptides oligomers. Interesting observations can be made, concerning the hydrazidic *Z*/*E* isomerism, by comparison of the NMR data between aza-β^3-peptides oligomers of increasing length and the model compounds **1c** and **1d**.

The spectrum of dimer **2a** shows two sets of signals. For the major conformer (78%), the hydrazidic NH appears at 9.01 ppm and the corresponding carbonyl carbon appears at 167.93 ppm. The latter value clearly attests for *Z* geometry. The difference of around 2.50 ppm between the chemical shift value of the hydrazidic NH in **2a** (9.01 ppm) and the reference value of free hydrazidic NH measured from **1a** or **1c** (~6.50 ppm, *Z*-isomer) is very close to the $\Delta\delta$ value of 2.60 ppm observed for **1c**. This implies that the hydrazidic NH of the major conformer of **2a** is involved in a N—N-turn. For the minor conformer (22%), for which diastereotopic signals are observed, the corresponding values of 7.19 ppm (7.21 ppm for **1b**) and 174.35 ppm indicates an *E* geometry with a weak H-bond contact between the hydrazidic NH and the ester group. The analysis of the equilibrium is summarized in Figure 11.

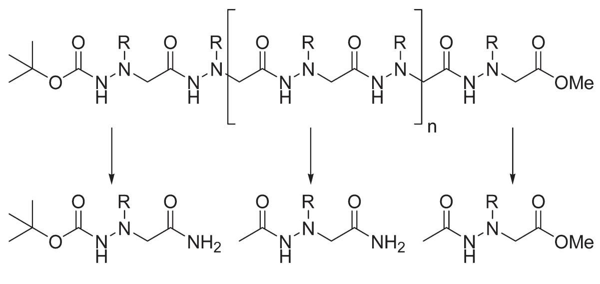

Figure 4. Chemical structures of model compounds **1b**, **1c**, and **1d**.

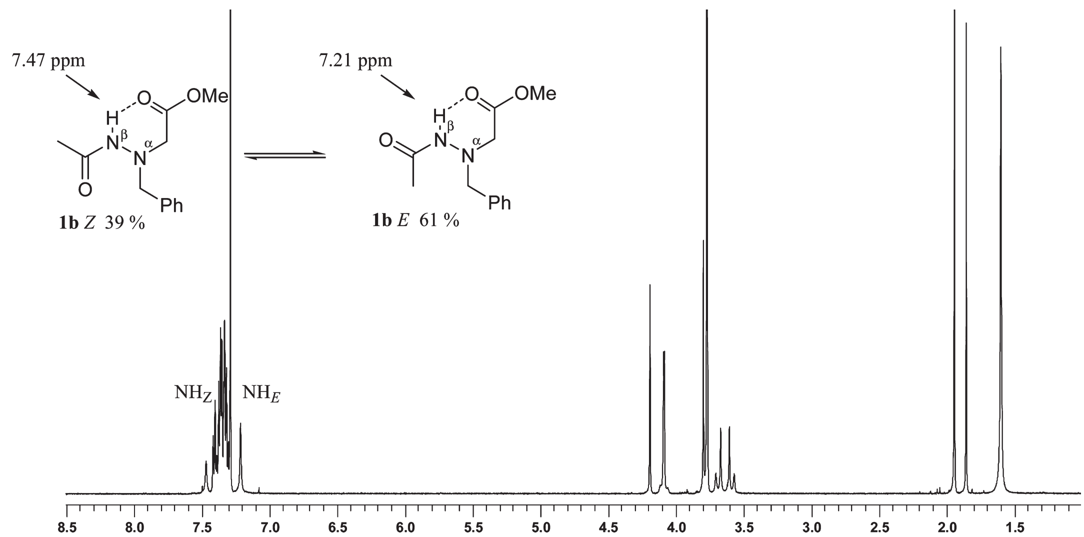

Figure 5. ^{1}H NMR (500 MHz) spectrum of **1b** (T = 298 K/10 mM/$CDCl_3$) corresponding to the conformational equilibrium of model compound **1b** ($CDCl_3$).

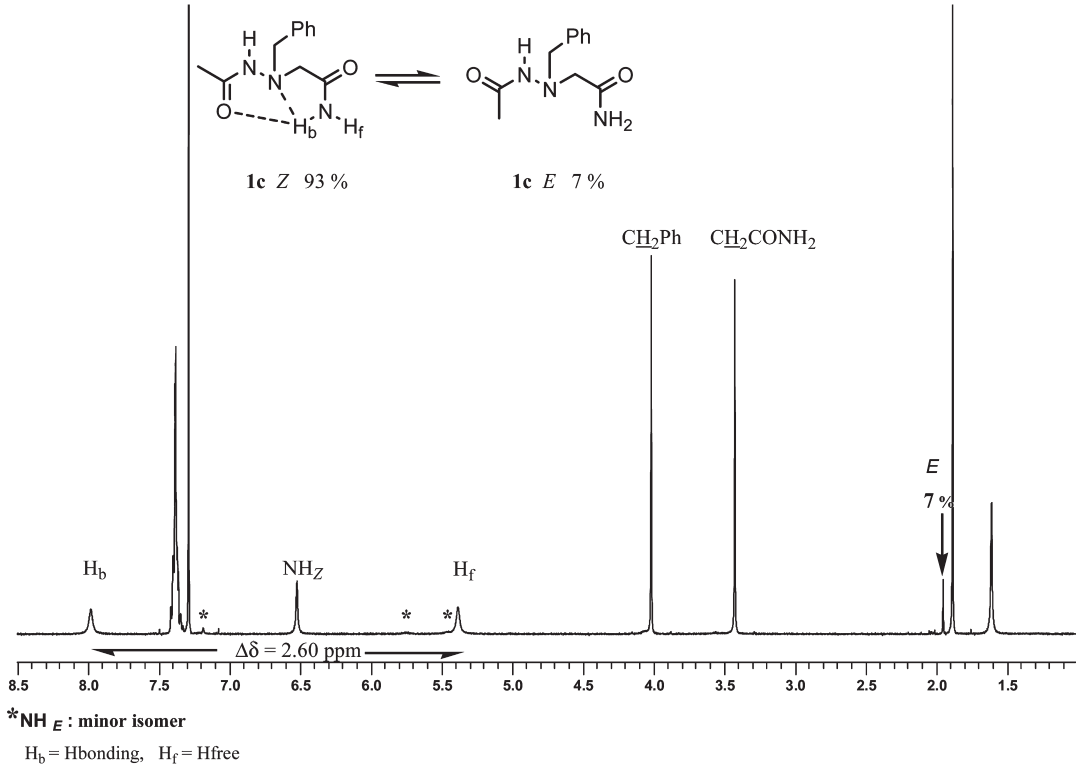

Figure 6. ^{1}H NMR (500 MHz) spectrum of **1c** (T = 298 K/10 mM/$CDCl_3$).

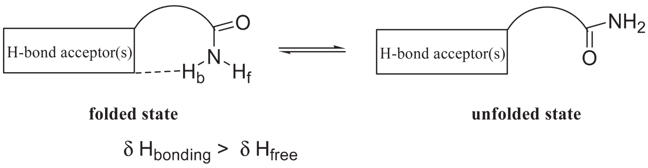

Figure 7. Equilibrium between the folded and unfolded state governed by intramolecular H-bonding in primary amides.

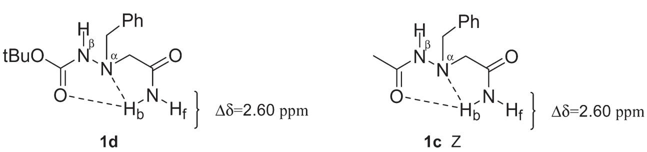

Figure 8. Discrimination of amidic protons through H-bonding in **1c** and **1d**.

For dimer **2b**, a single set of signals is observed, with a hydrazidic NH at 9.22 ppm, a hydrazidic carbonyl group at 168.99 ppm, and a $\Delta\delta$ value of 2.96 ppm. These data are directly transposable into a double hydrazinoturn conformation. The higher value of the hydrazidic chemical shift and the higher $\Delta\delta$, relative to **1c** (Z geometry), very probably reflects the cooperative effect of the H-bond network (Figure 12).

In a longer aza-β^3-peptides ester, the amount of the E form decreases very rapidly. The tetramer **3a**, which is the upper limit of detection of the E form at the C-terminus, provides a case study. The major form is a Z^4 conformer with three hydrazinoturns (all hydrazidic NHs between 9.11 and 9.66 ppm and all hydrazidic carbonyl carbons between 168 and 169 ppm). The minor set of signals corresponds to a Z^3E conformer (5%), where a residual Z/E isomerism is still detectable for the hydrazidic bond located at the C-terminus (Figure 13). For upper homologues ($n > 4$), only the Z^n conformation is detectable. We assume that the rapid extinction of the E form signals in the ester series results from H-bond cooperativity.

***Z/E* Isomerism of the Amidoxy Bond.** Given the structural relationship between the hydrazide bond and the amidoxy bond, it was interesting to apply the previous analysis to the latter. Compounds **1e**, **1f** and **1g** were thus synthesized (Figure 14).

The spectra of compound **1e** and **1f** show similar features. Both are poorly resolved at 298 K but can be analyzed at 278 K. At this temperature, two sets of signals are observed in 70:30 and 85:15 ratios for **1e** and **1f**, respectively (Figures 15 and 16). The 2D-HMBC sequence reveals that the carbonyl group of the amidoxy bond appears at 168.23 ppm for the major form of **1e** (168.41 for **1f**) and 175 ppm for the minor one (175.44 for **1f**). Moreover, like in the Z-isomer of compound **1b**, no $^{3}J_{CH}$ coupling is observed between the NH signal (9.04 ppm) and the carbon of the methyl group in the major isomer of **1f** (Figure 16). It is clear that, in contrast to **1b**, the Z form of the amidoxy bond largely predominates for **1e** and **1f** in $CDCl_3$. This experimental result diverges somewhat with the theoretical approach of Yang who predicted the E-form to be slightly preferred in these conditions. It is thus not surprising that only one conformer is observed for **1g**. Indeed, since we have seen that the formation of a N−N-turn can reverse the Z/E equilibrium in **1b** (39:61) to a 93:7 Z/E ratio in **1c**, one would predict that, starting from a more favorable ratio, the equilibrium will be totally shifted to the Z isomer for **1g**, and indeed this occurs (Figure 17).

The comparison of the ^{1}H NMR spectra of **1b** (Figure 5) and **1f** (Figure 16) reveals that the double bond character is somewhat

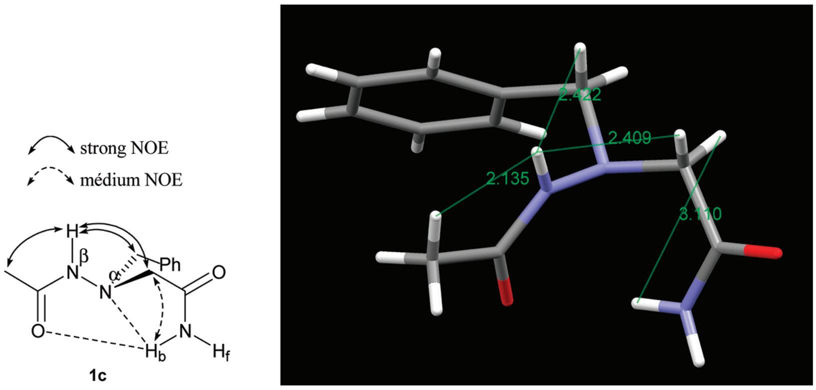

Figure 9. (Left) Summary of the NOEs observed for **1c** (10 mM in $CDCl_3$). (Right) Selected interatomic distances (in Å) observed in the solid state of **1c**.

Table 1. ^{13}C NMR Chemical Shift of the Carbonyl Group in the *Z* and *E* Isomers 1a−c (10 mM in $CDCl_3$)

	Z-Isomer δCO_h (ppm)	*E*-Isomer δCO_h (ppm)
1a	169.68	175.47
1b	169.17	175.38
1c	169.58	174.41

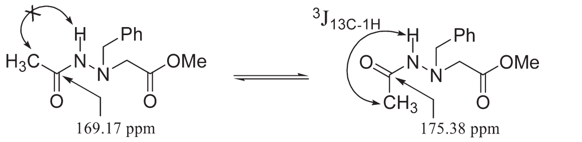

1b *Z* 39% **1b** *E* 61%

Figure 10. NMR discrimination between the *Z* and *E* rotamers of **1b**.

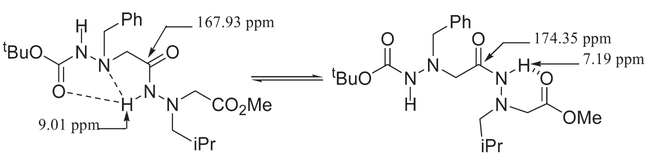

2a *Z* 78% **2a** *E* 22%

Figure 11. Conformational equilibrium of dimer **2a** (10 mM in $CDCl_3$).

lower for the amidoxy bond as attested by the coalescence of signals of the *E* and *Z* isomer at 298 K. Possibly, the electron-withdrawing effect of the adjacent oxygen atom limits the conjugative effect. Consequently, the amidoxy carbonyl group is a weaker H-bond acceptor compared to the hydrazidic carbonyl group. As the $\Delta\delta$ values remain of the same order in **1c** (2.60 ppm) and **1g** (2.70 ppm), it is likely that the N−O turn, like the N−N-turn, is stabilized by a XHY bifurcated H-bond.[16] On the other hand, the higher chemical shift value of the amidoxy NH in **1g** (8.41 ppm versus 6.52 ppm for the hydrazidic NH in **1c**) reflects its stronger acidity, once again in relation with the adjacent electron-withdrawing oxygen atom.

As expected, hybrid oligomers consisting of alternated α-aminoxyacids and aza-β^3-aminoacids behave very closely with pure aza-β^3-peptides, showing the same strong preference for the Z^n conformation (this is evidenced in Supporting Information, S33).

2b

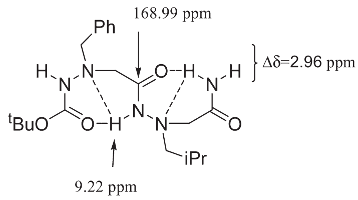

Figure 12. Ground conformation of dimer **2b** (10 mM in $CDCl_3$).

Finally, we applied our criterions to the hybrid cyclohexamer **4** (Figure 18). In this macrocycle, broad signals are observed for methylene protons of the aza-β^3-peptidic unit at 298 K, which resolve into AB systems at 258 K (Figure 18, right). The ^{13}C assignment reveals hydrazidic and amidoxy carbonyl carbon at 168.50 ppm and 167.67 ppm, respectively, which indicates *Z* geometry for both. The hydrazido and amidoxy NHs appear strongly deshielded at 10.64 and 11.57 ppm (Figure 18, left). All these elements are fully compatible with a conformation where N−N and N−O turns alternate.

The crystal structure of **4** fits very well with the conformational preference in solution, showing a fully interconnected H-bond network sustained by both type of pseudocycles. The comparison with the solid state conformation of the corresponding aza-β^3-cyclohexapeptidic[17] backbone illustrates their very close geometry (Figure 19).

We have previously shown that the diastereotopic signals observed in the case of aza-β^3-cyclohexapeptides result from a strong lowering of the pyramidal inversion rate.[17] Hybrid compound **4** reproduces this phenomenon with a lower energy barrier because of the lower steric crowding resulting from the lack of side chain on the aminoxyacid units. The nonambiguous conformation adopted by **4** indicates that the empirical rule, which associates diastereotopy with the *E*-geometry of a hydrazidic bond, cannot be used for macrocyclic derivatives and makes the new criterion we have identified all the more relevant.

■ CONCLUSIONS

The present study sheds light on the *Z*/*E* isomerism of both hydrazide and amidoxy bonds. It puts forward new NMR tools that can potentially be used to discriminate *E* and *Z* isomers associated with the hydrazidic and amidoxy bond, namely, the difference in chemical shift between the carbonyle in the *Z*-isomer (around or below 170 ppm) and in the *E*-isomer (around 175 ppm) and the

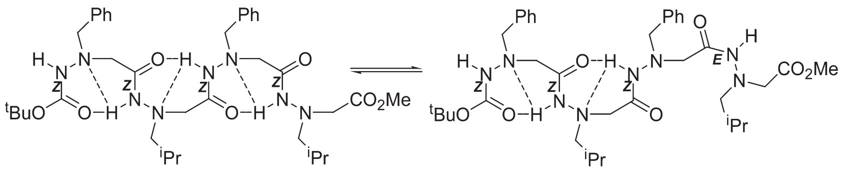

3a Z^4 95% **3a** Z^3E 5%

Figure 13. Conformational equilibrium of tetramer 3 (10 mM in $CDCl_3$).

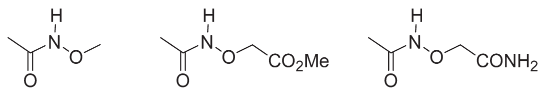

1e **1f** **1g**

Figure 14. Chemical structures of model compounds **1e**−**g**.

existence of a $^3J_{1H13C}$ coupling between the NH proton and the carbon atom in the α position of the carbonyle. It shows that the double bond character of the CO−NH bond is somewhat lower in the amidoxy bond, probably due to the electron-withdrawing effect of the adjacent oxygen atom, but that the amidoxy NH is correlatively more acidic. Both aza-β^3-aminoacids and α-aminoxyacids are prone to stabilize bifurcated 8-membered hydrogen-bonded pseudocycles, namely, the so-called N−N and N−O turn, which share very similar characteristics. α-Aminoxy-peptides are better preorganized to sustain such H-bond network as the amidoxy bond revealed a natural preference for the *Z* geometry in $CDCl_3$. Finally, the cooperativity effect associated with the network of N−N-turns rapidly decreases the amount of residual *Z*/*E* isomerism at the C-terminus of aza-β^3-peptides.

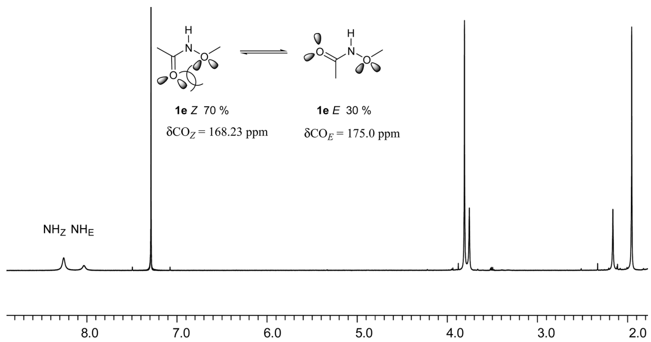

Figure 15. ^{1}H NMR (500 MHz) spectrum of **1e** (T = 278 K/10 mM/$CDCl_3$).

EXPERIMENTAL SECTION

General Methods. All chemicals and solvents were of laboratory grade from commercial suppliers and were used without further purification. Silica gel chromatography was performed with silica gel 60 (particle size 40−63 μm). ^{1}H and ^{13}C NMR were measured on a 500 MHz (500 MHz for ^{1}H, and 125 MHz for ^{13}C), a 300 MHz (300 MHz for ^{1}H; 75 MHz for ^{13}C) or a 200 MHz (200 MHz for ^{1}H; 50 MHz for ^{13}C) NMR spectrometer. Chemical shifts (δ) are reported in parts per million (ppm) for ^{1}H and for ^{13}C NMR spectra. Coupling constants (J) are reported in hertz (Hz). High-resolution mass spectrometric analyses were performed with an ESI source and were carried out at the CRMPO (Centre Regional de Mesures de l'Ouest) of Rennes, France.

General Procedure for Saponification. To a solution of ester (x mmol) in acetonitrile (20 mL/10 mmol of ester) was added NaOH 2 N (1.2.x mmol). The mixture was stirred for 3 h at room temperature. After evaporation of acetonitrile, the residue was diluted with 30 mL of water, washed twice with ether (2 × 30 mL), acidified by addition of HCl 2 N, and extracted with DCM (2 × 50 mL). The combined extracts were dried over Na_2SO_4. Filtration and evaporation of the solvent afforded the corresponding acid.

General Procedure for Boc Deprotection. A solution of the Boc-protected ester, typically 10 mmol in DCM (4 mL) and TFA (6 mL) was stirred for 3 h at room temperature. After dilution with water (30 mL) and DCM (30 mL), $NaHCO_3$ 1 N was added under vigorous stirring until pH 7−8 was reached and stabilized. The organic layer was dried (Na_2SO_4), and the solvent was removed in vacuo to afford the corresponding free amino ester.

General Coupling Procedure. All coupling steps leading to aza-β^3-peptides or hybrid oligomers were performed using the EDC/HOBT (1.2 eq relative to the acid) activation in DCM. The mixture was stirred for 12 h. The organic layer was washed successively twice with 15 mL of 1 N HCl, twice with 15 mL of water, and twice with 15 mL of 1 N $NaHCO_3$, dried on Na_2SO_4 and evaporated.

***N'*-*N'*-Dibenzyl-acethydrazide (1a).** **1a** was prepared following the work of N. Prasad.[18] ^{1}H NMR (500 MHz, $CDCl_3$/298 K) δ (ppm) major isomer: (E: 74%) 1.70 (s, 3H, CH_3), 3.71 (d, J = 10.67 Hz, 2H, 2 × CH_A), 3.98 (d, J = 10.67 Hz, 2H, 2 × CH_B), 6.05 (s, 1H, NH), 7.30−7.40 (m, 10H, 2 × C_6H_5). Minor isomer: (Z: 26%) 1.75 (s, 3H, CH_3), 4.23 (s, 4H, 2 × CH_2), 7.30−7.40 (m, 6H, 4 × CH_m, 2 × CH_p), 7.41 (d, J = 7.16 Hz, 4H, 4 × CH_o). ^{1}H NMR (500 MHz, $CDCl_3$/318 K) δ major isomer (E: 74%): 1.71 (s, 3H, CH_3), 3.74 (sl, 2H, $2CH_A$), 3.95 (sl, 2H, 2 × CH_B), 6.02 (s, 1H, NH), 7.30−7.41 (m, 10H, 2 × C_6H_5). Minor isomer (*Z*: 26%): 1.74 (s, 3H, CH_3), 4.23 (s, 4H, 2 × CH_2), 6.50 (sl, 1H, NH), 7.30−7.41 (m, 10H, 2 × C_6H_5). ^{1}H NMR (500 MHz, DMSO-d_6/298 K) δ major isomer (*E*: 53%): 1.34 (s, 3H, CH_3), 3.72 (d, J = 12.49 Hz, 2H, 2 × CH_A), 3.92 (d, J = 12.49 Hz, 2H, 2 × CH_B), 7.24−7.37 (m, 10H, 2 × C_6H_5), 8.19 (s, 1H, NH). Minor isomer (*Z*: 47%): 1.58 (s, 3H, CH_3), 4.00 (s, 4H, 2 × CH_2), 7.24−7.37 (m, 10H, 2 × C_6H_5), 8.80 (s, 1H, NH). ^{13}C NMR (50 MHz, $CDCl_3$) δ major isomer: 20.11 (CH_3), 63.1 (2 × CH_2), 128.3 (2 × CH_p), 128.9 (4 × CH), 130.2 (4 × CH), 136.4 (2 × C), 175.5 (CO). Minor isomer: 21.9 (CH_3), 59.8 (2 × CH_2), 127.9 (2 × CH_p), 128.8 (4 × CH), 129.6 (4 × CH), 137.8 (2 × C), 169.7 (CO).

Synthesis of Ac-(aza-*β*^{3}-Phe)-OMe (1b). Thionyl chloride (3.40 g; 28.56 mmol) was added dropwise to a solution of Boc-(aza-β^3-Phe)−OH (4.00 g; 14.28 mmol) in methanol (30 mL).[4a] The mixture was stirred for 12 h at room temperature. Evaporation of solvent and trituration of the residue in ether gave quantitatively HCl·H-(aza-β^3-Phe)-OMe as a white powder. The latter was dissolved in a mixture of DCM (40 mL) and Et_3N (2.88 g; 28.56 mmol). After cooling to 0 °C, a solution of acetyl chloride (1.00 g; 12.74 mmol) in ethyl ether (30 mL) was added dropwise. The mixture was allowed to warm to room temperature and stirred for 3 h. Solvent was removed, and

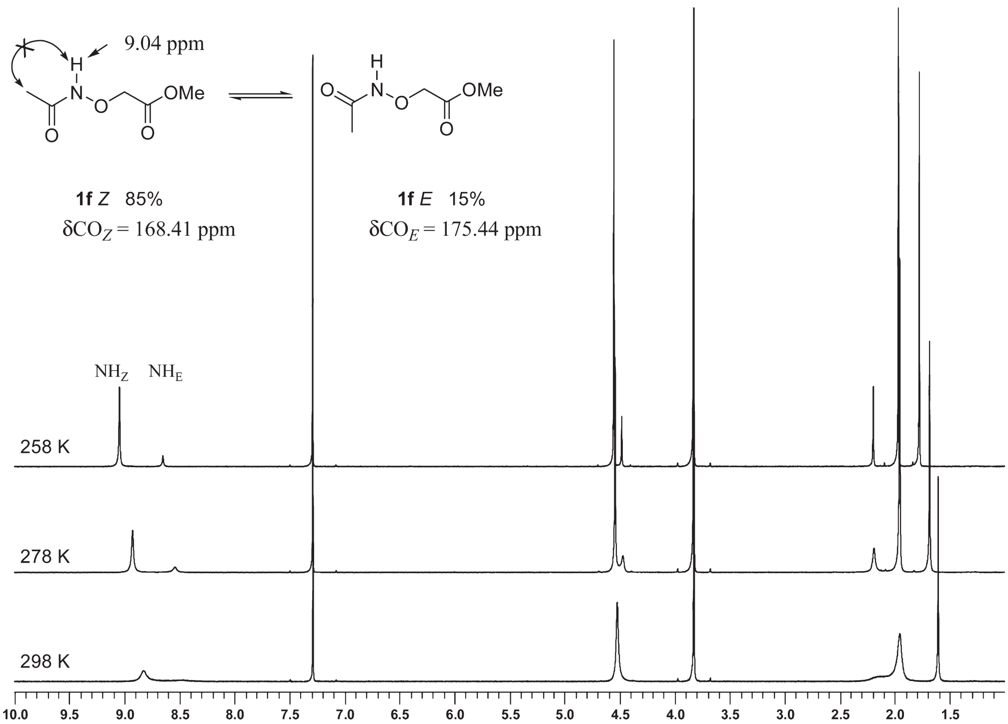

Figure 16. [1]H NMR (500 MHz of **1f** (20 mM in $CDCl_3$, at 298 K; 278 K; 258 K).

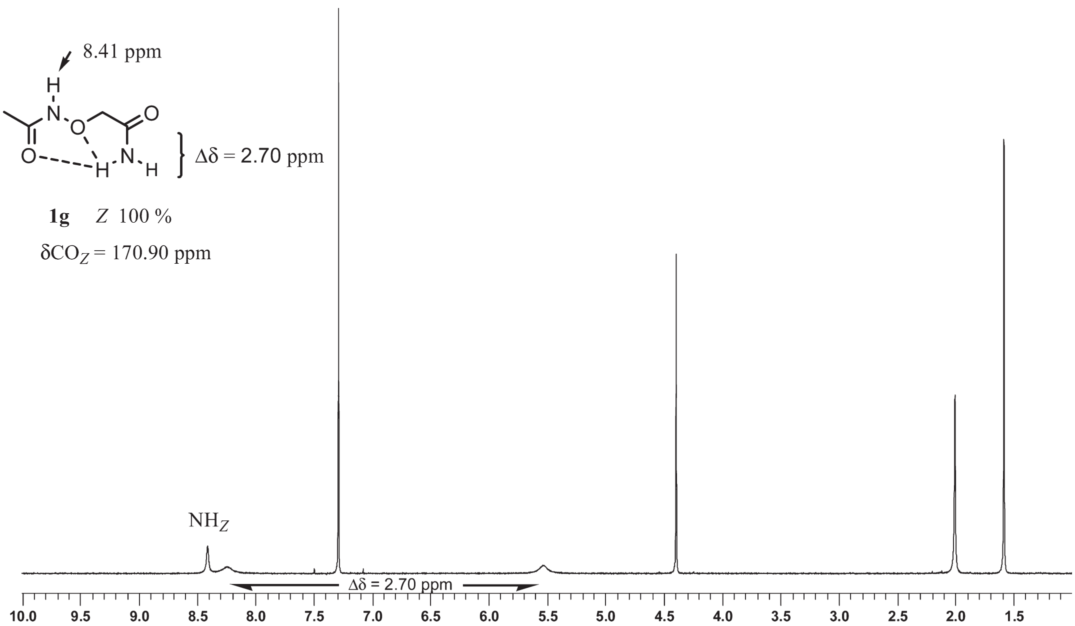

Figure 17. [1]H NMR (500 MHz) spectrum of **1g** (T = 298 K/10 mM/$CDCl_3$).

EtOAc (20 mL) was added to the residue. The precipitated $NEt_3 \cdot HCl$ was filtered and solvent was evaporated to give a crude oil that was dissolved in DCM (50 mL). The organic layer was washed successively twice with 15 mL of 1 N HCl, twice with 15 mL of water, twice with 15 mL of 1 N $NaHCO_3$, and dried on Na_2SO_4. After solvent evaporation, the oily residue was purified by column chromatography on silica gel (EtOAc) to afford **1b** as a colorless oil (2.42 g; 72%): [1]H NMR (500 MHz, $CDCl_3$/298 K) δ major isomer (E: 61%): 1.94 (s, 3H, CH_3), 3.59 (d, J = 17.48 Hz, 1H, CH), 3.68 (d, J = 17.48 Hz, 1H, CH), 3.77 (s, 3H, CH_3), 4.08 (d, J = 12.29 Hz, 1H, CH), 4.09 (d, J = 12.29 Hz, 1H, CH), 7.21 (s, 1H, NH), 7.30−7.39 (m, 5H, C_6H_5). Minor isomer (Z: 39%): 1.85 (s, 3H, CH_3), 3.76 (s, 3H, CH_3), 3.79 (s, 2H, CH_2), 4.19 (s, 2H, CH_2), 7.30−7.39 (m, 3H, 2 × CH_m, CH_p), 7.41 (d, J = 7.01 Hz, 2H, 2 × CH_o), 7.47 (s, 1H, NH). [13]C NMR (50 MHz, $CDCl_3$/298 K) δ major isomer: 19.9 (CH_3), 52.1 (CH_3), 57.0 (CH_2), 62.1 (CH_2), 128.3 (CH_p), 128.9 (2 × CH_m), 130.0 (2 × CH_o), 136.06 (C), 170.5 (CO), 175.4 (CO). Minor isomer: 21.8 (CH_3), 52.0 (CH_3), 55.4 (CH_2), 60.1 (CH_2), 127.9 (CH_p), 128.7 (2 × CH_m), 129.4 (2 × CH_o), 136.8 (C), 169.2

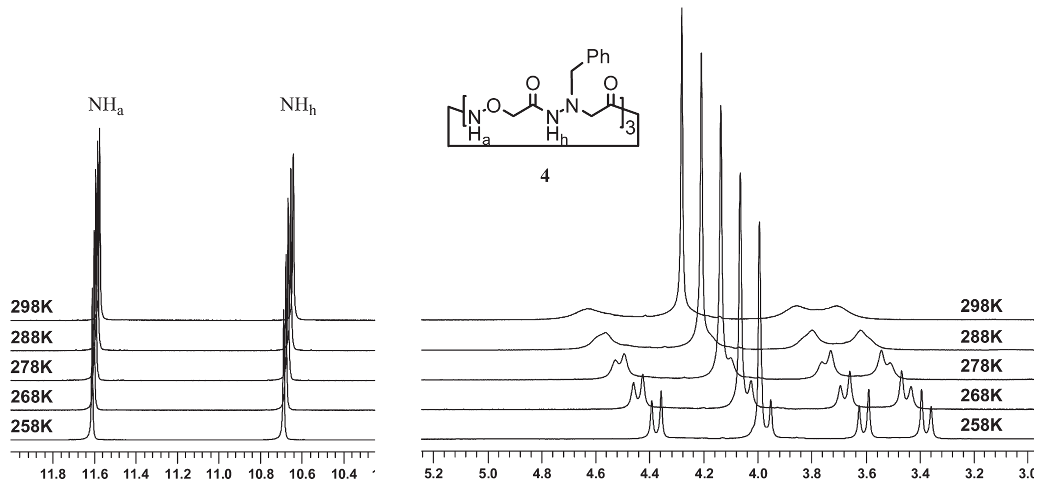

Figure 18. ^{1}H NMR (500 MHz) spectrum of **4** (T = 298 to 258 K/10 mM/$CDCl_3$).

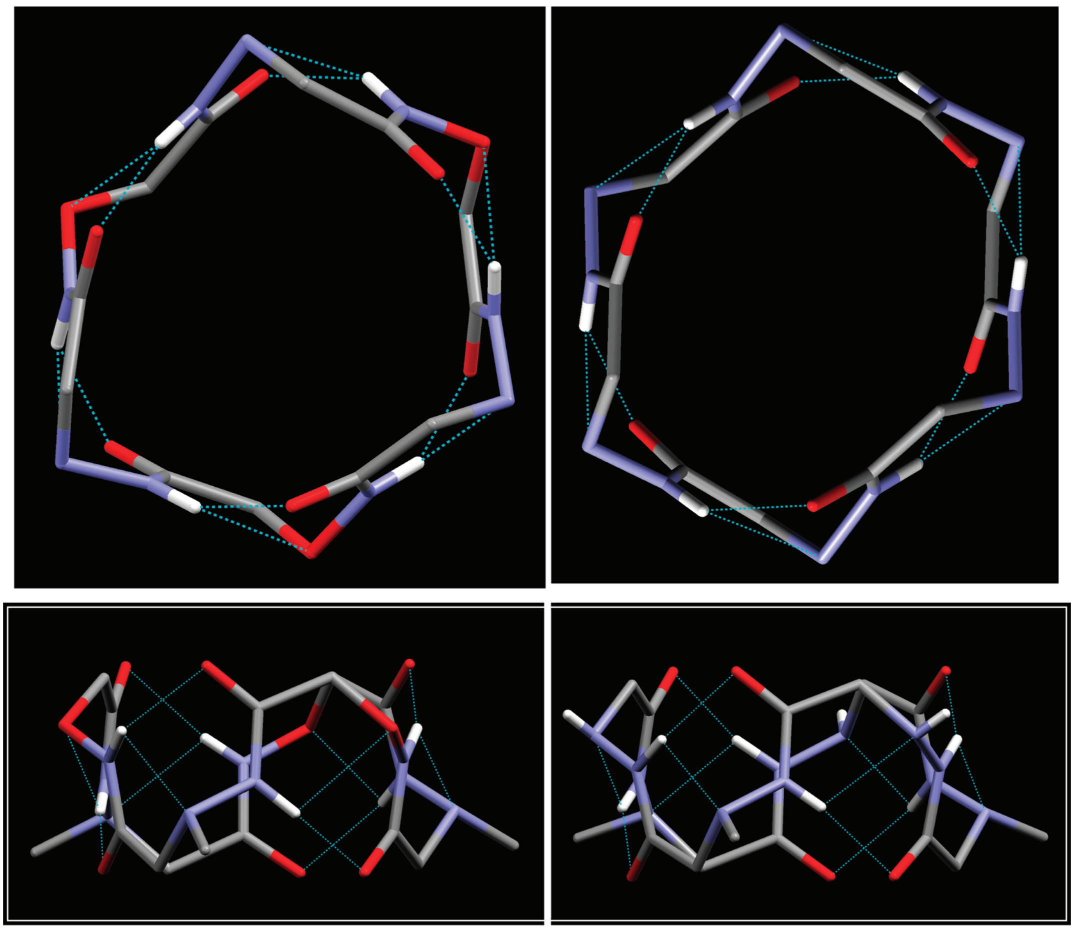

Figure 19. Juxtaposition showing the very close analogy observed in the solid state between the conformation of the backbone in hybrid cyclohexamer **4** (left) and pure aza-β^3-cyclohexapeptides (right) (H-bonds in dotted lines; hydrogen atoms except the NHs have been deleted; side chains have been replaced by carbon atoms on bottom views).

(CO), 171.7 (CO). HRMS (ESI) Calcd for $C_{12}H_{16}N_2O_3Na$ 259.1059; Found, 259.1061.

Synthesis of Ac-(aza-β^3-Phe)-NH$_2$ (1c). Compound Ac-(aza-β^3-Phe)-OMe **1b** (1.00 g; 4.24 mmol) was dissolved in 7N ammonia solution in methanol (20 mL). The mixture was stirred for 12 h at room temperature. Excess of NH_3/MeOH was eliminated under vacuo. Trituration in ether and filtration gave Ac-(aza-β^3-Phe)-NH$_2$ **1c** as a white solid (mp = 163 °C) (0.87 g; 93%). ^{1}H NMR (500 MHz, $CDCl_3$/298K) δ major isomer (Z, 93%): 1.88 (s, 3H, CH_3), 3.42 (s, 2H, CH_2), 4.02 (s, 2H, CH_2Ph), 5.38 (s, 1H, NH), 6.52 (s, 1H, NH hydrazidique), 7.34−7.41 (m, 5H, C_6H_5), 7.98 (s, 1H, NH). Minor isomer (E, 7%): 1.95 (s, 3H, CH_3), 5.45 (s, 1H, NH), 5.75 (s, 1H, NH), 7.18 (s, 1H, NH

dx.doi.org/10.1021/jo201390b |J. Org. Chem. 2011, 76, 8756–8767

hydrazidic). ^{13}C NMR (50 MHz, $CDCl_3$) δ major isomer 21.7 (CH_3), 60.0 (CH_2), 63.3 (CH_2), 128.8 (CH_p), 129.2 (2 × CH), 129. Nine (2 × CH), 135.2 (C), 169.6 (CO), 172.7 (CO). Minor isomer: 20.2 (CH_3), 174.4 (CO). HRMS (ESI) Calcd for $C_{11}H_{15}N_3O_2Na$ 244.1062; Found, 244.1062.

Boc-(aza-β^3-Phe)-NH$_2$ (1d). **1d** was obtained as described in our previous work.[7c] ^{1}H NMR 500 MHz (10 mM, $CDCl_3$) δ 1.39 (s, 9H, 3 × CH_3), 3.40 (s, 2H, CH_2), 3.98 (s, 2H, CH_2), 5.40 (broad, 1H, NH), 5,67 (s, 1H, NH), 7.33−7.38 (m, 5H,), 8.00 (broad, 1H, NH).

Synthesis of Ac-NH-OMe (1e). At 0 °C, acetyl chloride (2.25 g, 28.7 mmol) and Et_3N (3.62 g, 35.9 mmol) were successively added dropwise to a solution of methoxylamine hydrochloride (2 g, 23 mmol) in DCM. The mixture was allowed to warm to room temperature and stirred for 12 h. After evaporation of solvent, the residue was triturated in diethylether and filtrated. The oily residue was purified by column chromatography on silica gel (Et_2O (100%), then EtOAc (100%), then MeOH/EtOAc (10/90) and MeOH (100%) to afford **1e** as incolor oil (1.6 g; 70%). ^{1}H NMR (500 MHz, $CDCl_3$/278 K) δ major isomer (*Z*: 70%): 1.95 (s, 3H, CH_3), 3.81 (s, 3H, CH_3), 8.26 (s board, 1H, NH). Minor isomer (*E*: 30%): 2.16 (s, 3H, CH_3), 3.76 (s, 3H, CH_3), 8.03 (s board, 1H, NH). ^{13}C NMR (50 MHz, $CDCl_3$) δ major isomer: 19.7 (CH_3), 64.2 (CH_3), 168.2 (CO). Minor isomer: 19.0 (CH_3), 64.8 (CH_3). HRMS (ESI) Calcd for $C_3H_7N_1O_2Na$ 112.0374; Found, 112.0374.

Synthesis of Ac-NH−OCH$_2$CO$_2$Me (1f). To tert-butyl *N*-hydroxycarbamate (3.50 g; 26.31 mmol) and benzyl-bromoacetate (6.02 g; 26.31 mmol) in DCM (80 mL) was added K_2CO_3 (3.63 g; 26.31 mmol). The mixture was stirred for 72 h at room temperature. After filtration, the organic layer was concentrated in vacuo to give quantitatively Boc-NH−OCH_2CO_2Bn as an oil. ^{1}H NMR (200 MHz, $CDCl_3$) δ: 1.49 (s, 9H, 3 × CH_3), 4.50 (s, 2H, CH_2), 5.23 (s, 2H, CH_2Ph), 7.39 (s, 5H, C_6H_5), 7.78 (s, 1H, NHBoc). Compound Boc-NH−OCH_2CO_2Bn (7.40 g; 26.31 mmol) was dissolved in 60 mL of isopropanol. Pd/C (10%, 500 mg) was added, and the mixture was stirred for 12 h under hydrogen atmosphere. After filtration on Celite, isopropanol was evaporated. The crude acid was precipitated by trituration in an ether/pentane mixture (70/30). Filtration gave monomer Boc-NH−OCH_2CO_2H (3.6 g; 73%). ^{1}H NMR (200 MHz, $CDCl_3$) δ: 1.52 (s, 9H, 3 × CH_3), 4.51 (s, 2H, CH_2), 8.05 (s, 1H, NHBoc), 8.80 (sl, 1H, OH). Thionyl chloride (2.86 g; 24.08 mmol) was added dropwise to a solution of Boc-NH−OCH_2CO_2H (2.30 g; 12.04 mmol) in methanol (30 mL). The mixture was stirred for 12 h at room temperature. Evaporation of the methanol afforded quantitatively the hydrochloride HCl, H_2N-OCH_2CO_2Me as a solid. ^{1}H NMR (200 MHz, D_2O) δ: 3.74 (s, 3H, CH_3), 4.65 (s, 2H, CH_2). To a solution of the hydrochloride (1.70 g; 12.04 mmol) in DCM (30 mL) was added Et_3N (2.50 g; 24.75 mmol). The mixture was cooled to 0 °C, and acetyl chloride (950 mg; 12.04 mmol) in ethyl ether (30 mL) was added dropwise. The mixture was allowed to warm to room temperature and stirred for 4 h. The solvent was removed in vacuo and EtOAc (10 mL) was added to the residue. The salt of Et_3N was filtered and solvent was evaporated. The crude oil was purified by column chromatography on silica gel using (EtOAc/ethanol: 90/10) to give **1f** as a white solid (mp = 91−93 °C), (0.79 g; 45%). ^{1}H NMR (500 MHz, $CDCl_3$/298 K) δ 1.90−2.30 (sl, 3H, CH_3), 3.83 (s, 3H, CH_3), 4.52 (s, 2H, CH_2), 8.30−9.00 (sl, 1H, NH). ^{1}H NMR (500 MHz, $CDCl_3$/258 K) δ major isomer (*Z*: 85%) 1.97 (s, 3H, CH_3), 3.83 (s, 3H, CH_3), 4.55 (s, 2H, CH_2), 9.04 (s, 1H, NH). Minor isomer (*E*: 15%) 2.20 (s, 3H, CH_3), 3.83 (s, 3H, CH_3), 4.48 (s, 2H, CH_2), 8.65 (s, 1H, NH). ^{13}C NMR (50 MHz, $CDCl_3$/298 K) δ: 19.98 (CH_3), 52.41 (CH_3), 72.56 (CH_2), 168.73 (CO), 170.35 (CO). ^{13}C NMR (125 MHz, $CDCl_3$/263 K) δ major isomer 20.5 (CH_3), 52.96 (CH_3), 72.5 (CH_2), 168.4 (CO), 170.7 (CO). Minor isomer 20.5 (CH_3), 52.9 (CH_3), 73.3 (CH_2), 169.8 (CO), 175.4 (CO). HRMS (ESI) Calcd for $C_5H_9N_1O_4Na$ 170.0429; Found, 170.0427.

Synthesis of Ac-NH−OCH$_2$CONH$_2$ (1g). Monomer **1f** (300 mg; 2.04 mmol) was dissolved in a 7N Ammonia solution in methanol. The mixture was stirred for 12 h at room temperature. Excess of NH_3/MeOH was evaporated in vacuo. The crude solid was triturated in ether. Filtration gave **1g** as a white solid (mp = 90−92 °C), (250 mg; 93%). ^{1}H NMR (500 MHz, $CDCl_3$) δ: 2.00 (s, 3H, CH_3), 4.39 (s, 2H, CH_2), 5.54 (sl, 1H, NH), 8.24 (sl, 1H, NH), 8.41 (s, 1H, NH). ^{13}C NMR (125 MHz, $CDCl_3$) δ 20.1 (CH_3), 76.5 (CH_2), 170.9 (CO), 171.5 (CO). HRMS (ESI) Calcd for $C_4H_8N_2O_3Na$ 155.0433; Found, 155.0434.

Synthesis of Boc-(aza-β^3-Phe)-(aza-β^3-Leu)-OMe (2a). The general coupling procedure was applied to obtain compound **2a**. Coupling of monomer Boc-(aza-β^3-Phe)−OH (3.00 g; 10.71 mmol) and monomer H-(aza-β^3-Leu)-OMe (2.05 g; 12.86 mmol) afforded dimer **2a**. The crude dimer was precipitated in an ether/pentane mixture. Filtration of solid gave **2a** (mp = 110 °C) (3.61 g; 80%). ^{1}H NMR (500 MHz, $CDCl_3$) δ major isomer (78%): 0.94 (d, *J* = 6.62 Hz, 6H, 2 × CH_3), 1.41 (s, 9H, 3 × CH_3), 1.68 (n, *J* = 6.80 Hz, 1H, CH), 2.75 (d, *J* = 7.11 Hz, 2H, CH_2), 3.43 (s, 2H, CH_2), 3.72 (s, 2H, CH_2), 3.78 (s, 3H, CH_3), 3.99 (s, 2H, CH_2), 5.83 (s, 1H, NH), 7.27−7.38 (m, 5H, C_6H_5), 9.01 (s, 1H, NH). Minor isomer (22%): 0.76 (d, *J* = 6.26 Hz, 6H, 2 × CH_3), 1.44 (s, 10H, 3 × CH_3, CH), 2.48 (dd, *J* = 12.53 Hz, *J* = 7.66 Hz, 1H, CH), 2.62 (dd, *J* = 12.44 Hz, *J* = 6.35 Hz, 1H, CH), 3.42 (d, *J* = 17.68 Hz, 1H, CH), 3.49 (d, *J* = 17.68 Hz, 1H, CH), 3.74 (s, 3H, CH_3), 3.75 (d, *J* = 17.62 Hz, 1H, CH), 3.82 (d, *J* = 17.62 Hz, 1H, CH), 4.20 (s, 2H, CH_2), 5.83 (s, 1H, NH), 7.19 (s, 1H, NH), 7.27−7.38 (m, 3H, 2 × CH_m, CH_p), 7.45 (d, *J* = 7.05 Hz, 2H, 2 × CH_o). ^{13}C NMR (50 MHz, $CDCl_3$) δ major isomer: 21.0 (2 × CH_3), 27.0 (CH), 28.6 (3 × CH_3), 52.0 (CH_3), 58.3 (CH_2), 59.8 (CH_2), 63.1 (CH_2), 64.8 (CH_2), 80.9 (C), 128.4 (CH_p), 128.9 (2 × CH_m), 129.9 (2 × CH_o), 135.9 (C), 155.5 (CO), 167.9 (CO), 171.2 (CO). Minor isomer: 20.6 (2 × CH_3), 26.6 (CH), 28.7 (3 × CH_3), 52.2 (CH_3), 53.9 (CH_2), 57.6 (CH_2), 60.9 (CH_2), 66.1 (CH_2), 80.1 (C), 127.9 (CH_p), 128.7 (2 × CH_m), 129.9 (2 × CH_o), 137.7 (C), 155.5 (CO), 170.7 (CO), 174.3 (CO). HRMS (ESI) Calcd for $C_{21}H_{34}N_4O_5Na$ 445.2427; Found, 445.2428.

Synthesis of Boc-(aza-β^3-Phe)-(aza-β^3-Leu)-NH$_2$ (2b). Dimer Boc-(aza-β^3-Phe)-(aza-β^3-Leu)-OMe **2a** was dissolved in Ammonia, ca. 7N solution in methanol (20 mL). The mixture was stirred for 48 h at room temperature. Excess NH_3/MeOH was concentrated in vacuo. The crude solid was triturated in ether. Filtration gave **2b** as a white solid (mp = 156−158 °C), (86%). ^{1}H NMR (500 MHz, $CDCl_3$) δ: 0.97 (d, *J* = 6.60 Hz, 6H, 2 × CH_3), 1.37 (s, 9H, 3 × CH_3), 1.61 (n, *J* = 6.78 Hz, 1H, CH), 2.61 (d, *J* = 7.21 Hz, 2H, CH_2), 3.40 (s, 2H, CH_2), 3.43 (s, 2H, CH_2), 3.94 (s, 2H, CH_2), 5.38 (s, 1H, NH), 5.64 (s, 1H, NH), 7.34−7.40 (m, 5H, C_6H_5), 8.34 (s, 1H, NH), 9.22 (s, 1H, NH). ^{13}C NMR (75 MHz, $CDCl_3$) δ: 20.9 (2 × CH_3), 26.8 (CH), 28.6 (3 × CH_3), 59.9 (CH_2), 62.2 (CH_2), 63.9 (CH_2), 67.6 (CH_2), 81.5 (C), 128.5 (CH_p), 128.9 (2 × CH_m), 129.9 (2 × CH_o), 135.4 (C), 156.5 (CO), 169.0 (CO), 173.4 (CO). HRMS (ESI) Calcd for $C_{20}H_{33}N_5O_4Na$ 430.2430; Found, 430.2428.

Synthesis of 3. Coupling of dimer Boc-(aza-β^3-Phe-aza-β^3-Leu)−OH (2.32 g; 5.68 mmol) and dimer H-(aza-β^3-Phe-aza-β^3-Leu)-OMe (1.83 g; 5.68 mmol) afforded tetramer as an amorphous solid after evaporation. Solubilized in ether, the crude tetramer precipitated after trituration. Two filtrations gave tetramer **3** (3.23 g, 80%). ^{1}H NMR (500 MHz, $CDCl_3$) δ 0.91 (d, *J* = 6.60 Hz, 6H, 2 × CH_3), 0.93 (d, *J* = 6.68 Hz, 6H, 2 × CH_3), 1.35 (s, 9H, 3 × CH_3), 1.54 (n, *J* = 6.83 Hz, 1H, CH), 1.58 (n, *J* = 6.64 Hz, 1H, CH), 2.51 (d, *J* = 7.15 Hz, 2H, CH_2), 2.72 (d, *J* = 7.01 Hz, 2H, CH_2), 3.29 (s, 2H, CH_2), 3.34 (s, 2H, CH_2), 3.44 (s, 2H, CH_2), 3.68 (s, 2H, CH_2), 3.78 (s, 3H, CH_3), 3.88 (s, 2H, CH_2), 3.94 (s, 2H, CH_2), 5.53 (s, 1H, NH), 7.23−7.43 (m, 10H, 2 × C_6H_5), 9.13 (s, 1H, NH), 9.42 (s, 1H, NH), 9.66 (s, 1H, NH). ^{13}C NMR (50 MHz, $CDCl_3$) δ: 20.9 (2 × CH_3), 21.1 (2 × CH_3), 26.8 (CH), 26.9 (CH), 28.6 (3 × CH_3), 51.9 (CH_3), 58.8 (CH_2), 60.0 (CH_2), 60.1 (CH_2), 61.9 (CH_2), 62.8 (CH_2), 63.9 (CH_2), 64.7 (CH_2), 67.5 (CH_2), 81.6 (C), 127.9 (CH_p), 128.6 (CH_p), 128.7 (2 × CH_m), 128.9 (2 × CH_m), 129.3

(2 × CH_o), 130.0 (2 × CH_o), 134.9 (C), 136.9 (C), 156.5 (CO), 167.9 (CO), 168.5 (CO), 169.0 (CO), 171.0 (CO).

Synthesis of Macrocycle 4. The synthesis leading to the hybrid oligomer precursor of macrocycle **4** was performed using the general procedures. The synopsis of the synthetic route leading to compound **4** is reported in Supporting Information S30. These products were roughly purified and used as such.

Compound Boc-(αO-Gly-aza-β^3-Phe)-OMe a (oil). ^{1}H NMR (500 MHz, $CDCl_3$) δ (ppm) major isomer (60%): 1.50 (s, 9H, 3 × CH_3), 3.78 (s, 3H, CH_3), 3.79 (s, 2H, CH_2), 4.23 (s, 2H, CH_2), 4.28 (s, 2H, CH_2), 7.27−7.44 (m, 5H, C_6H_5), 7.45 (s, 1H, NH), 8.98 (s, 1H, NH). Minor isomer (40%): 1.48 (s, 9H, 3 × CH_3), 3.55 (d, J = 17.77 Hz, 1H, CH), 3.65 (d, J = 17.77 Hz, 1H, CH), 3.77 (s, 3H, CH_3), 4.02 (d, J = 12.61 Hz, 1H, CH), 4.06 (d, J = 12.61 Hz, 1H, CH), 4.24 (d, J = 16.65 Hz, 1H, CH), 4.65 (d, J = 16.65 Hz, 1H, CH), 7.27−7.44 (m, 5H, C_6H_5), 7.44 (s, 1H, NH), 8.04 (s, 1H, NH). ^{13}C NMR (75 MHz, $CDCl_3$) δ major isomer: 28.6 (3 × CH_3), 52.2 (CH_3), 55.9 (CH_2), 60.6 (CH_2), 76.1 (CH_2), 83.3 (C), 128.2 (CH_p), 128.9 (2 × CH_m), 129.7 (2 × CH_o), 136.8 (C), 157.5 (CO), 167.2 (CO), 171.3 (CO). Minor isomer: 28.7 (3 × CH_3), 52.4 (CH_3), 56.7 (CH_2), 62.2 (CH_2), 73.3 (CH_2), 82.0 (C), 128.9 (CH_p), 129.3 (2 × CH_m), 130.1 (2 × CH_o), 135.6 (C), 156.4 (CO), 170.5 (CO), 172.8 (CO).

Compound Boc-(αO-Gly-aza-β^3-Phe)−OH b (White Solid from Ether). ^{1}H NMR (300 MHz, $CDCl_3$) δ (ppm): 1.50 (s, 9H, 3 × CH_3), 3.63 (s, 2H, CH_2), 4.11 (s, 2H, CH_2), 4.32 (s, 2H, CH_2), 7.31−7.42 (m, 5H, C_6H_5), 7.62 (s, 1H, NH), 10.04 (s, 1H, NH).

Compound $_2$HN-(αO-Gly-aza-β^3-Phe)-OMe c (Oil). ^{1}H NMR (200 MHz, $CDCl_3$) δ (ppm) major isomer (60%): 3.76 (s, 3H, CH_3), 3.82 (s, 2H, CH_2), 4.08 (s, 2H, CH_2), 4.21 (s, 2H, CH_2), 7.28−7.44 (m, 5H, C_6H_5), 8.19 (s, 1H, NH). Minor isomer (40%): 3.52 (d, J = 17.66 Hz, 1H, CH_A), 3.68 (d, J = 17.66 Hz, 1H, CH_B), 3.76 (s, 3H, CH_3), 4.02 (d, J = 12.11 Hz, 1H, CH_{A1}), 4.10 (d, J = 12.11 Hz, 1H, CH_{B1}), 4.10 (d, J = 16.65 Hz, 1H, CH_{A2}), 4.50 (d, J = 16.65 Hz, 1H, CH_{B2}), 7.28−7.44 (m, 6H, C_6H_5, NH).

Compound Boc(α-OGly-aza-β^3-Phe)$_2$OMe d (Solid from Ether). ^{1}H NMR (500 MHz, $CDCl_3$,10^{-2} M/298K) δ (ppm): 1.52 (s, 9H, 3 × CH_3), 3.44 (s, 2H, CH_2), 3.74 (s, 3H, CH_3), 3.75 (s, 2H, CH_2), 3.95 (s, 2H, CH_2), 4.20 (s, 2H, CH_2), 4.25 (s, 2H, CH_2), 4.31 (s, 2H, CH_2), 7.21−7.41 (m, 10H, 2 × C_6H_5), 7.59 (s, 1H, NH), 9.57 (s, 1H, NH), 9.76 (s, 1H, NH), 11.37 (s, 1H, NH). ^{13}C NMR (75 MHz, $CDCl_3$) δ (ppm): 28.5 (3 × CH_3), 52.1 (CH_3), 56.2 (CH_2), 59.4 (CH_2), 60.3 (CH_2), 63.4 (CH_2), 76.0 (CH_2), 76.0 (CH_2), 84.0 (C), 127.9 (CH_p), 128.6 (CH_p), 128.7 (2 × CH_m), 129.0 (2 × CH_m), 129.5 (4 × CH_o), 135.6 (C), 136.9 (C), 158.8 (CO), 167.0 (CO), 169.0 (CO), 169.4 (CO), 170.9 (CO).

Compound $_2$HN-(α-OGly-aza-β^3-Phe)$_2$OMe e (Foam). ^{1}H NMR (200 MHz, $CDCl_3$) δ: (ppm): 3.41 (s, 2H, CH_2), 3.74 (s, 3H, CH_3), 3.76 (s, 2H, CH_2), 3.95 (s, 2H, CH_2), 4.07 (s, 2H, CH_2), 4.20 (s, 2H, CH_2), 4.32 (s, 2H, CH_2), 7.21−7.43 (m, 11H, 2 × C_6H_5, NH), 9.52 (s, 1H, NH), 11.13 (s, 1H, NH).

Macrocycle **4** was obtained using a final high dilution intramolecular coupling step (1 mM) as follows. 670 mg (0.81 mmol) of Boc(α-OGly-aza-β^3-Phe)$_3$OH was treated with a mixture of DCM/TFA (6 mL/4 mL) during 12 h. The excess of TFA was then coevaporated under reduced pressure with toluene (3 × 20 mL) then ether (3 × 20 mL) until a white foam appeared. The crude residue was dissolved in 20 mL of DCM and 10 mmol of triethylamine was added. This solution was poured drop by drop into a solution of EDCI (8 mmol) and HOBT (8 mmol) in 1.5 L of DCM. The reaction was stirred vigorously for 72 h (unoptimized). The volume was then reduced to around 100 mL. The addition of 20 mL of 1 N HCl under stirring gave rise to the apparition of a white solid (HOBT, HCl), which was filtrated by suction. The solution was then washed successively with 20 mL of 1 N HCl, twice with 20 mL of water, and twice with 20 mL of 1 N $NaHCO_3$ and evaporated. The crude reaction product was obtained as an off-white powder (315 mg, 55%). Crystals have been grown from EtOAc (mp > 260 °C). ^{1}H NMR (500 MHz, $CDCl_3$, $CDCl_3$/10^{-2} M/258K) δ (ppm): 3.38 (d, J = 17.46 Hz, 3H, 3 × CH), 3.60 (d, J = 17.46 Hz, 3H, 3 × CH), 3.97 (d, J = 17.34 Hz, 3H, 3 × CH), 3.99 (s, 6H, 3 × CH_2), 4.37 (d, J = 17.34 Hz, 3H, 3 × CH), 7.33−7.37 (m, 15H, 3 × C_6H_5), 10.69 (s, 3H, 3 × NH), 11.61 (s, 3H, 3 × NH). RMN ^{13}C (75 MHz, $CDCl_3$) δ (ppm): 58.7 (3 × CH_2), 64.1 (3 × CH_2), 76.0 (3 × CH_2), 128.8 (3 × CH_p), 129.1 (6 × CH_m), 129.7 (6 × CH_o), 135.3 (3 × C), 167.7 (3 × CO), 168.5 (3 × CO). HRMS (ESI) Calcd for $C_{33}H_{39}N_9O_9Na$ 728.2768; Found, 728.2774.

■ ASSOCIATED CONTENT

Ⓢ Supporting Information. Copies of ^{1}H NMR and ^{13}C NMR spectroscopic data for compounds **1a**−**g**, **2a**−**b**, **3**, **4** and precursors of **4**. Synopsis of the synthetic route leading to compound **4**. Portions of the ^{2}D-HMBC spectrum and the summary of NOEs observed for compound **1b**, **1c**, and **1g** in $CDCl_3$ at 298 K and for compound **1f** at 263 K. Portions of the ^{2}D-HMQC spectrum and the summary of NOEs observed for compound **1g** in $CDCl_3$ at 298 K. Portions of the ^{2}D-NOESY spectrum and the summary of NOEs observed for compounds **1a** in DMSO-d_6 at 298 K and **1c** in $CDCl_3$ at 298 K. Crystallographic data in CIF format for compounds **1c** and **4**. This material is available free of charge via the Internet at http://pubs.acs.org.

■ AUTHOR INFORMATION

Corresponding Author
*philippe.legrel@univ-rennes1.fr

■ ACKNOWLEDGMENT

We are grateful for the support provided by ANR (National Research Agency).

■ REFERENCES

(1) (a) Gellman, S. H. *Acc. Chem. Res.* **1998**, *31*, 173. (b) Hill, D. J.; Mio, M. J.; Prince, R. B.; Hughes, T. S.; Moore, J. S. *Chem. Rev.* **2001**, *101*, 3893. (c) Hecht, S.; Huc, I. *Foldamers: Structure, Properties, and Applications*; Wiley: New York, 2007.

(2) (a) Semetey, V.; Rognan, D.; Hemmerlin, C.; Graff, R.; Briand, J.-P.; Marraud, M.; Guichard, G. *Angew. Chem., Int. Ed.* **2002**, *41*, 1893. (b) Violette, A.; Fournel, S.; Lamour, K.; Chaloin, O.; Frisch, B.; Briand, J.-P.; Monteil, H.; Guichard, G. *Chem. Biol.* **2006**, *13*, 531.

(3) (a) Yang, D.; Qu, J.; Li, B.; Ng, F.-F.; Wang, X.-C.; Cheung, K.-K.; Wang, D.-P.; Wu, Y. D. *J. Am. Chem. Soc.* **1999**, *121*, 589–590. (b) Yang, D.; Li, B.; Ng, F.-F.; Yan, Y.-L.; Qu, J.; Wu, Y.-D. *J. Org. Chem.* **2001**, *66*, 7303. (c) Peter, C.; Daura, X.; van Gunsteren, W. F. *J. Am. Chem. Soc.* **2000**, *122*, 7461.

(4) (a) Cheguillaume, A.; Salaün, A.; Sinbandhit, S.; Potel, M.; Gall, P.; Baudy-Floc'h, M.; Le Grel, P. *J. Org. Chem.* **2001**, *66*, 4923. (b) Salaün, A.; Potel, M.; Roisnel, T.; Gall, P.; Le Grel, P. *J. Org. Chem.* **2005**, *70*, 6499.

(5) (a) Zuckermann, R. N.; Kerr, J. M.; Kent, S. B. H.; Moos, W. H. *J. Am. Chem. Soc.* **1992**, *114*, 10646. (b) Hamper, B. C.; Kolodziej, S. A.; Scates, A. M.; Smith, R. G.; Cortez, E. *J. Org. Chem.* **1998**, *63*, 708. (c) Roy, O.; Faure, S.; Thery, V.; Didierjean, C.; Taillefumier, C. *Org. Lett.* **2008**, *10*, 921.

(6) Han, H.; Janda, K, D. *J. Am. Chem. Soc.* **1996**, *118*, 2539.

(7) (a) Yang, D.; Ng, F.-F.; Li, Z.-J.; Wu, Y. D.; Chan, K. W.K.; Wang, D.-P. *J. Am. Chem. Soc.* **1996**, *118*, 9794. (b) Thévenet, L.; Vanderesse, R.; Marraud, M.; Didierjean, C.; Aubbry, A. *Tetrahedron. Lett.* **2000**,

41, 2361. (c) Salaün, A.; Favre, A.; Le Grel, B.; Potel, M.; Le Grel, P. *J. Org. Chem.* **2006**, *71*, 150.
(8) Hobohm, U.; Sander, C. *Protein Sci.* **1994**, *3*, 522–524.
(9) Poteau, R.; Trinquier, G. *J. Org. Chem.* **2007**, *72*, 8251–8258.
(10) (a) Anthoni, U.; Larsen, C.; Nielsen, P. H. *Acta Chem. Scand.* **1969**, *23*, 3513. (b) Walter, W.; Reubke, K.-J. *Chem. Ber.* **1970**, *103*, 2197. (c) Bouchet, P.; Elguero, J.; Jacquier, R.; Pereillo, J.-M. *Bull. Soc. Chim. Fr.* **1972**, *6*, 2264.
(11) Knapp, S.; Toby, B .H.; Sebastian, M.; Krogh-Jespersen, K.; Potenza, J. A. *J. Org. Chem.* **1981**, *46*, 2490.
(12) (a) Perdicchia, D.; Licandro, E.; Maiorana, S.; Baldoli, C.; Giannini, C. *Tetrahedron* **2003**, *59*, 7733. (b) Licandro, E.; Perdicchia, D. *Eur. J. Org. Chem.* **2004**, 665.
(13) Wu, Y. D.; Wang, D.-P.; Chan, K. W.K.; Yang, D. *J. Am. Chem. Soc.* **1999**, *121*, 11189–11196.
(14) Kopple, K. D.; Onishi, M.; Go, A. *Biochemistry* **1969**, *8*, 4087.
(15) Brown, A. C.; Guest, A. W.; Milner, P. H. *Tetrahedron Lett.* **1989**, *30*, 2433–2436.
(16) Yang, J; Gellman, S. H. *J. Am. Chem. Soc.* **1998**, *1201*, 9090–9091.
(17) Le Grel, P.; Salaün, A.; Potel, M.; Le Grel, B.; Lassagne, F. *J. Org. Chem.* **2006**, *71*, 5638.
(18) Prasad, D.; Sinha, V. N.; Prasad, N. *Nat. Acad. Sci. Lett.* **1985**, *8*, 115–118.